Iranian Journal of Physics Research, Vol. 25, No. 3, 2025
DOI: 10.47176/ijpr.25.3.32074

Simulation of lateral distribution function for proton and gamma ray extensive air showers from 1PeV to 100 EeV energy range

Zaynab Ali Nasser, Itab Fadhil Hussein*, and Ahmed Azeez Al-Rubaiee
Mustansiriyah University, College of Science, Department of Physics, Baghdad, Iraq

E-mail: itabfadhil@uomustansiriyah.edu.iq

(Received 13 March 2025 ; in final form 06 August 2025)

Abstract
This work investigates the properties of the Lateral Distribution Function (LDF) of gamma-ray-induced Extensive Air Showers (EAS) across a large energy range from (10^{15} to 10^{20}) eV, which includes the knee and ankle energy regions. The AIRES (AIR-shower Extended Simulations) system was used in simulations to generate secondary gamma rays, with primary protons serving as initiating particles. Hadronic interaction models, particularly QGSJET-04-II and EPOS-LHC, were used to explore the impact of alternative physical assumptions on shower development. The lateral distribution of secondary gamma rays was studied systematically at various primary energy and zenith angles. The findings show that the LDF is clearly dependent on primary energy, with considerable differences between the knee and ankle regions. Furthermore, zenith angles have a major influence on the lateral dispersion of gamma rays, emphasizing differences in particle interactions and shower dynamics. The sigmoidal function was used to set the lateral distribution coefficient curves of EAS, generating new coefficients as a function of primary energy. These findings provide vital insights into the behavior and detection of gamma-ray-induced EAS, increasing our knowledge of high-energy astrophysics and cosmic-ray studies.

Keywords: AIRES system, LDF, Ankle and Knee regions, Sigmoidal function.

1. Introduction

Cascade reaction EAS is used to identify high-energy cosmic rays (CRs) generated in the Earth's atmosphere due to their inability to directly detect some main particles. They need to be looked at based on measured showers in various ways when an atmospheric nucleus and a very high-energy cosmic ray collide. A collision results in many new energetic particles [1]. A considerable number of particles are added to the expanding cascade with each impact. They also strike air nuclei, a few particles that create neutral pions that immediately split into two gamma rays [2]. As they approach nuclei, the gamma rays create electron-positron pairs through bremsstrahlung; the electrons and positrons create gamma rays again, known as the electromagnetic cascade [3]. One of the most important features of an EAS is the Lateral Distribution function (LDF). Therefore, it is essential to define the LDF of the shower particles. The particle density or signal about the distance to the shower core location must be determined to calculate the cosmic ray energy with surface detection arrays [4,5,6]. Figure (1) displays the pattern diagram for the main processes in an extensive air shower, which form the hadronic, electromagnetic, muonic, and neutrino component. Electromagnetic, which is primarily composed of photons and electron positrons, is created with billions of particles and travels several kilometers before reaching the ground. Through fluorescence, these charged particles also produce ultraviolet light. Typically, the air shower is observed to make the primary UHECR observation.

About 40 years ago, during the cosmic ray flux, which was roughly $10^{15.5}$ eV was found in air shower size spectra, its power law spectrum showed a slight steepening. A range of interpretations were prompted, this spectral “knee,” which is yet unknown, and the ankle at $10^{18.5}$ eV was discovered more recently. Constitute A single characteristics in the high-energy incoming Spectrum of cosmic rays [8]. It has been established as a crucial area for additional cosmic-ray studies since the “knee” coincides with the highest energies anticipated from supernova remainders’ acceleration of diffusive shocks [9]. The knee is mostly generated by a break in the light primary spectra, where the cosmic rays’ average mass increases, according to several investigations [10, 11,12].

One of the broadest explanations for the knee’s Origin is that the strong SNR shock fronts are believed to have accelerated most cosmic rays, where the source exhibits a discernible split in the spectrum [13].

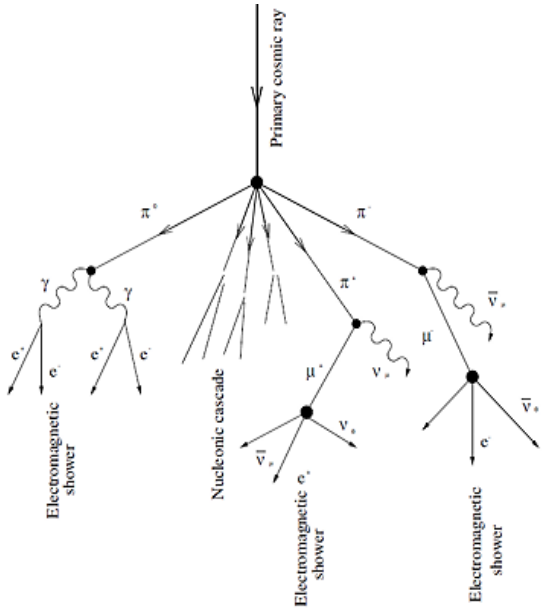

Figure 1. The pattern diagram for the development of the electromagnetic shower [7].

The knee's energy is around 4.10^{15} eV, perhaps around SNRs' magnitude (~ parsec). Proton steepening, an ankle-like structure, or a noticeable stiffening in the energy spectrum of cosmic ray light components at roughly 10^{17} eV were the three possible causes of the observed knee. According to this, cosmic rays might already be moving from their Origin in this muon and electron-proton energy spectrum from cosmic to extra-galactic [14]. F.Kadhom Fadhel, A. A. Al-Rubaiee, et al. investigated gamma-rays by simulating the LDF, which measures the number of charged particles, such as electron-positron couples and muons. that reach the Earth's surface and all other charged particles. The Monte Carlo AIRES system is used to accomplish this at ultrahigh energy (10^{16}, 10^{18}, and 10^{19} eV); the LDF was computed for various Nishimura–Kamata–Greisen (NKG) function and contrasted with the AIRES system simulation [15]. A. Geranios, E. Fokitis, et al. used the AIRES Monte Carlo program to model vertical EAS produced by a 100 EeV proton. The chosen energy is appropriate for detector arrays such as the P. Auger Observatory, where the Cerenkov detectors are 1.5 km apart [16]. A. Al-Rubaiee, U.Hashim, et al. employed parameterization to characterize the outcomes of the CORSIKA code numerical simulation of EAS of Cherenkov light released by EAS identified using the Tunka EAS apparatus, which is designed to investigate the mass composition and CRs' energy spectrum surrounding the knee region. The primary benefit of this method is its ability to recreate actual Cherenkov radiation events using the Tunka EAS array. It is possible to identify the main particle and compare the estimated Cherenkov light LDF to determine its energy surrounding the knee region. using the Tunka EAS Cherenkov array's reconstructed EAS events [17].

This study simulates significant gamma-ray air showers using the AIRES simulation system, which includes the QGSJET-04-II and EPOS-LHC models of hadronic interactions. Three main energies with three zenith angles in the knee and ankle portions of the cosmic ray spectrum are the subject of the analysis. To describe the behavior of the LDF and its dependence on the energy of the parent cosmic ray, coefficients of LDF are extracted from these simulations. These findings are essential for improving the accuracy of cosmic ray observations and expanding our knowledge of air shower formation.

Lateral Distribution Function:

One of the key features of ultra-high energy extended air showers that can be precisely measured by vast arrays of air showers on the ground is the local density of charged particles at different distances from the core site. Having precise theoretical predictions about the lateral distribution function (LDF) of different EAS components at a wide radial distance range is essential for both designing new tests and physically interpreting those that already exist [18,19]. Multiple scattering, air attenuation, and the production height distribution of the incoming particles all contribute to the lateral distributions [20]. Moreover, the EAS particles are generated using the transverse momentum distribution. As a result of the multiple scattering hypothesis, an accurate understanding of the lateral distribution of cascade showers is essential for the analysis of high-energy cosmic-ray events [21,22]. The lateral spread for medium air and the electron-photon component is estimated using the Moliere radius, which is r_0 = 9.6 g/cm^2, or 79 m at sea level. Studies have demonstrated that the shower's maximum height correlates with the LDF of Cherenkov radiation in an extensive air shower [23,24]. An atmospheric density distribution model can then translate the height to the atmospheric depth. Thus, the LDF of Cherenkov radiation can be used to estimate the shower's maximum depth [25]. For several reasons, it is essential to investigate the lateral distribution properties of EAS particles. First, modifications to the maximum shower development depth (X_{max}) with energy are reflected in their energy dependence. Second, a thorough examination of the LDF of the cascade particles within a specific energy range can provide a solid foundation for extending measurements into the area of ultra-high energy CR (UHECR), which currently lacks a wealth of experimental data [26,27]. However, at large values of age parameter (s), the NKG function will be very small at small distances from the axis, it still works well for $r > R_M$, r represents the distance from the core of the shower, $R_M = 78$m is the Moliere radius. Moreover, it reproduces the exact solution nicely at $0.6 < s < 1$. The link between the NKG function and the total number of electrons N_e at a specific depth is [28]:

$$\rho\left(\frac{r}{R_M}, N_e, E_\circ, s\right) = \frac{N_e}{2\pi R_M^2} C(S)\left(\frac{r}{R_M}\right)^{(S-2)} \times \left(\frac{r}{R_M}+1\right)^{(S-4.5)} \quad (1)$$

$\rho(r)$ is the density of electrons as a function of the distance from the core of the shower, N_e provides the total number of electrons present in the showers [29]:

$$N_e = 10^6\left(\frac{E_\circ}{10^{15}}\right)^{1.03} \quad (2)$$

The relation can represent the parameter (s) as the following [30].

$$s = \frac{3}{1+2B_\circ/t} \quad (3)$$

Where the atmospheric depth is represented by $B_\circ = \ln(E_\circ/\xi_c^e)$, ξ_c^e *is* critical energy of electron, $t = (x/x_\circ)\ln 2$ and the factor of normalization is $C(S)$ Given as follows [31]:

$$C(s) = 0.366s^2 \times (2.07 - s)^{1.25} \quad (4)$$

The primary energy, shower size, and the Moliere radius divided by the distance from the core shower, the NKG function in equation (1) is produced by the shower age parameter.

LDF Simulation Using AIRES System:

The Monte Carlo system is used to simulate the lateral dispersion of an extended air shower with a specific main particle type and energy based on a specific interaction model [32]. The AIRES system can examine the Earth's curvature and the properties of the geomagnetic field to provide full Particles moving across the atmosphere's real medium. The AIRES code was employed to simulate the LDF of generated particles in EAS, depicted as the photon density vs the core's distance [33]. The AIRES Monte Carlo code version 10.04.04 includes the models of high energy hadronic interactions EPOS_LHC [34] and QGSJET_04_II [35], which are used to simulate the EAS events. The telescope array (TA) data consists of a 1000 g/cm^2 slant depth and ground level (1,400 m above sea level). For primary proton-initiated gamma rays with energies of 10^{15}, 10^{18}, and 10^{20} eV at different zenith angles (0°, 15°, and 25°), with the thinning energy Rel: 10^{-6}, the lateral distribution simulation was performed.

Results and Discussion:

Simulation using AIRES code with primary proton revealed the distinct lateral distribution of secondary gamma rays across three energy 10^{15},10^{18}, 10^{20} eV and varying zenith angles.

From figures (2 and 3) Shows the correlation between the photon density logarithm as a function of the logarithmic core distance for primary protons at various energies (10^{15},10^{18} and 10^{20}) eV, displaying statistical uncertainty as error bars using the hadronic interaction models QGSJET-04-II and EPOS-LHC, considering various zenith angles (0°, 15°,25°). The photon density exhibits power-law behavior as the distance increases, higher primary energy results in a broader lateral spread, and greater photon density slows the drop over longer distances. The zenith angle also influences the density distribution; vertical showers (θ = 0°) have the highest density close to the core, but inclined showers (θ = 15°,25°) show a slower drop at further distances because of the longer atmospheric journey [36]. In contrast to EPOS-LHC, which predicts a more prolonged lateral spread, particularly at larger distances, and for tilted showers, QGSJET-04-II predicts somewhat higher particle concentrations at intermediate distances. Both models display comparable density patterns at the highest energy (10^{20} eV). Although the density distributions in the two models are comparable, these findings support the expected behavior of air showers and emphasize the need to use several hadronic models to improve air shower reconstruction methods and account for uncertainty in cosmic ray simulations [37,38]. In Figure (4**),** the comparison between QGSJET-04-II and EPOS-LHC shows noticeable differences in the lateral photon density distribution at medium energies (10^{15} -10^{18} eV), with a higher photon density predicted by EPOS-LHC at an extended distance from the core. Where the increased atmospheric depth alters the shower evolution. The results clearly show how the zenith angle affects things, as inclined showers θ =25° exhibit a shower decline in photon density compared to vertical showers θ = 0°. The longer atmospheric journey causes more interactions and energy losses before the photon reach the ground . However, at very high energies (10^{20}eV), the differences between the two models become less distinct, indicating that their results converge at these energies. This discrepancy at medium energies is attributed to differences in modeling hadronic interactions, particularly in forward particle production. The results highlight the need for additional experimental constraints to improve these models and ensure the accuracy of cosmic ray simulations.

Parameterization of LDF:

The photon's lateral distribution in EAS was analyzed applying a logistic function to the photon density description of the shower core's distance. The fitting process was conducted using the EPOS model. The study was performed at three energy levels and two zenith angles (0° and 25°).

The logistic function is denoted as:

$$\boldsymbol{\rho(x) = \lambda + \frac{(\alpha-\lambda)}{1+(\frac{x}{\eta})^{\beta}}} \quad (5)$$

Where:

$\rho(x)$ Represents the photon density in (photon/m^2), λ is the **photon density** at very large distances from the shower core, α is **the peak photon density** near the shower core η Controls on the **distance scale** at which the photon density transitions from peak α to λ. β the **steepness** of the photon density drop-off with distance, and x is a distance from the shower center in *m*. The corresponding values for these coefficients are displayed in Tables 1, 2, and 3.

Figure (5) illustrates the lateral distribution of photon density at different angles (0° and 25°) for proton primary particles with energies of 10^{15} eV, 10^{18} eV, and 10^{20} eV, respectively. The data symbols represent simulation results, while the lines correspond to fitted logistic functions using the EPOS_LHC model. Tables(1,2,3) accompanying each figure provide coefficients for the logistic functions, including coefficients such as α, λ, η, β, which characterize the distribution and the mean and SD can be used to illustrate the systematic uncertainty. In order to validate theoretical models against simulation data and comprehend the behavior of cosmic ray-induced air showers, these investigations are essential. The AIRES program was used to run the simulations, guaranteeing the results' high accuracy and dependability. Our knowledge of ultra-high energy cosmic rays and their interactions is expanded by this study.

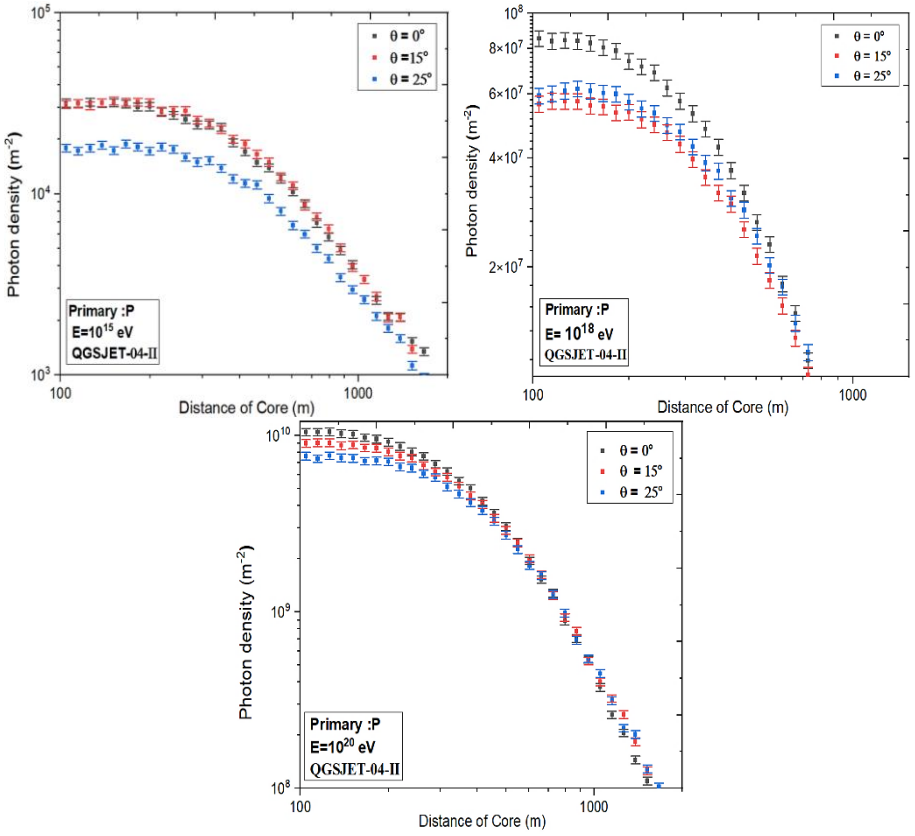

Figure 2. Lateral distribution of secondary photons produced from primary proton air showers simulated by QGSJET-04-II model at different primary energies and zenith angles.

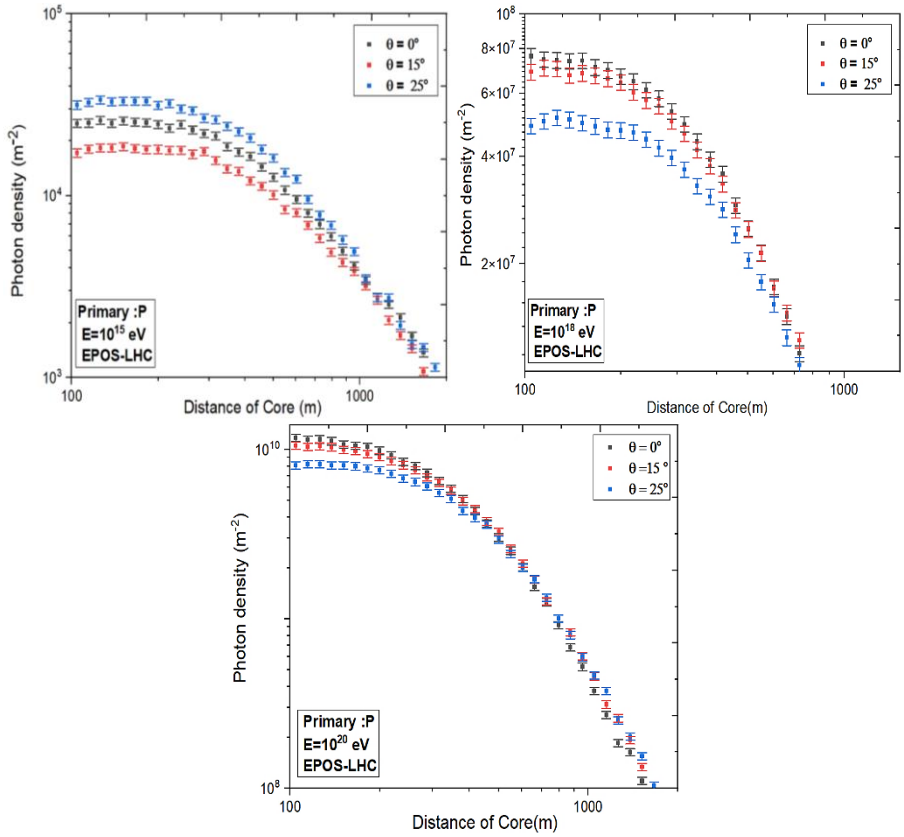

Figure 3. Lateral distribution of secondary photons produced from primary proton air showers simulated by EPOS-LHC model at

different primary energies and zenith angles.

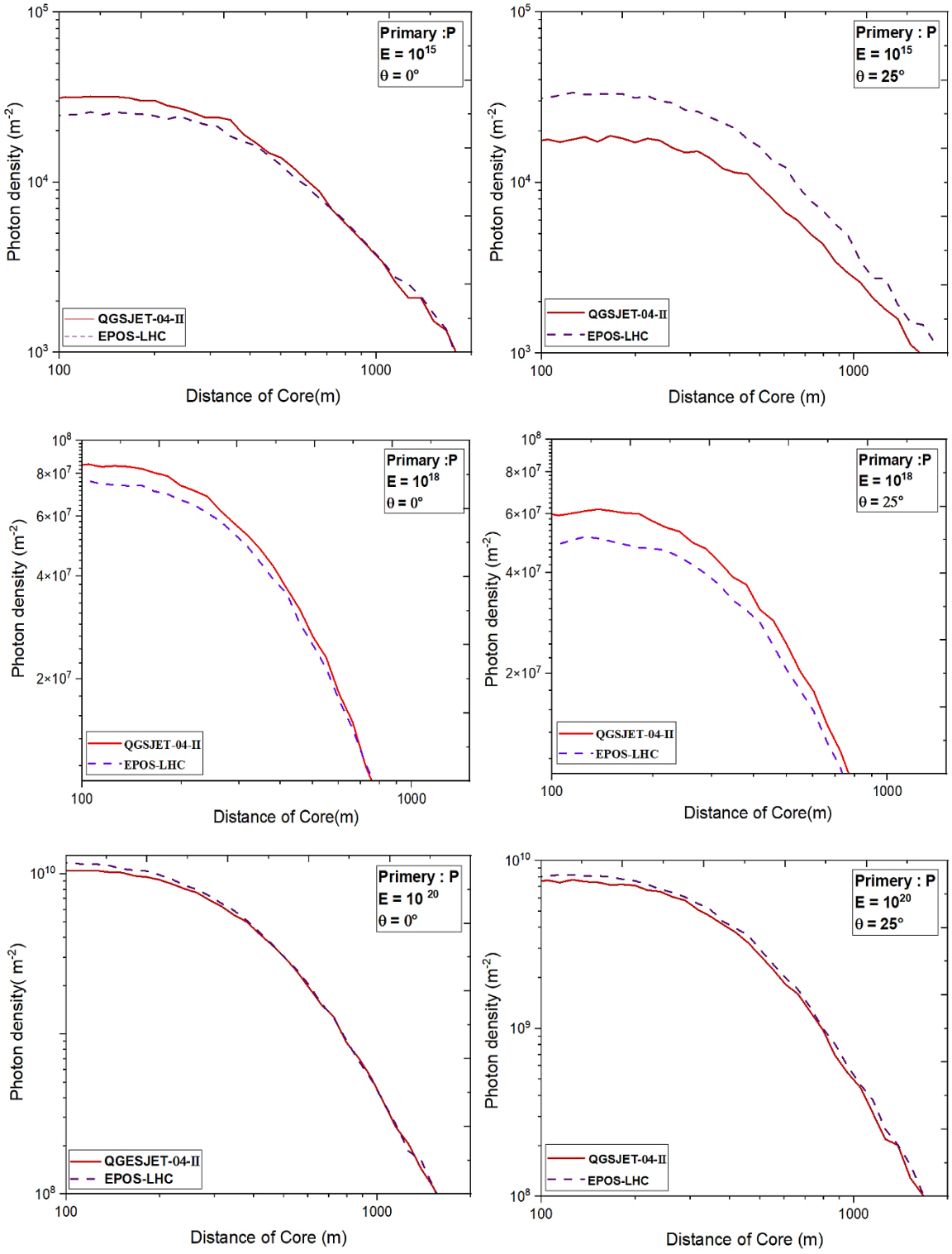

Figure 4. The simulation of lateral distributions function for proton primary using two models of hadronic interactions (EPOS-LHC, QGSJET-04-II) at the energies 10^{15}, $10^{18}$and 10^{20} eV with vertical and inclined showers (θ=25°).

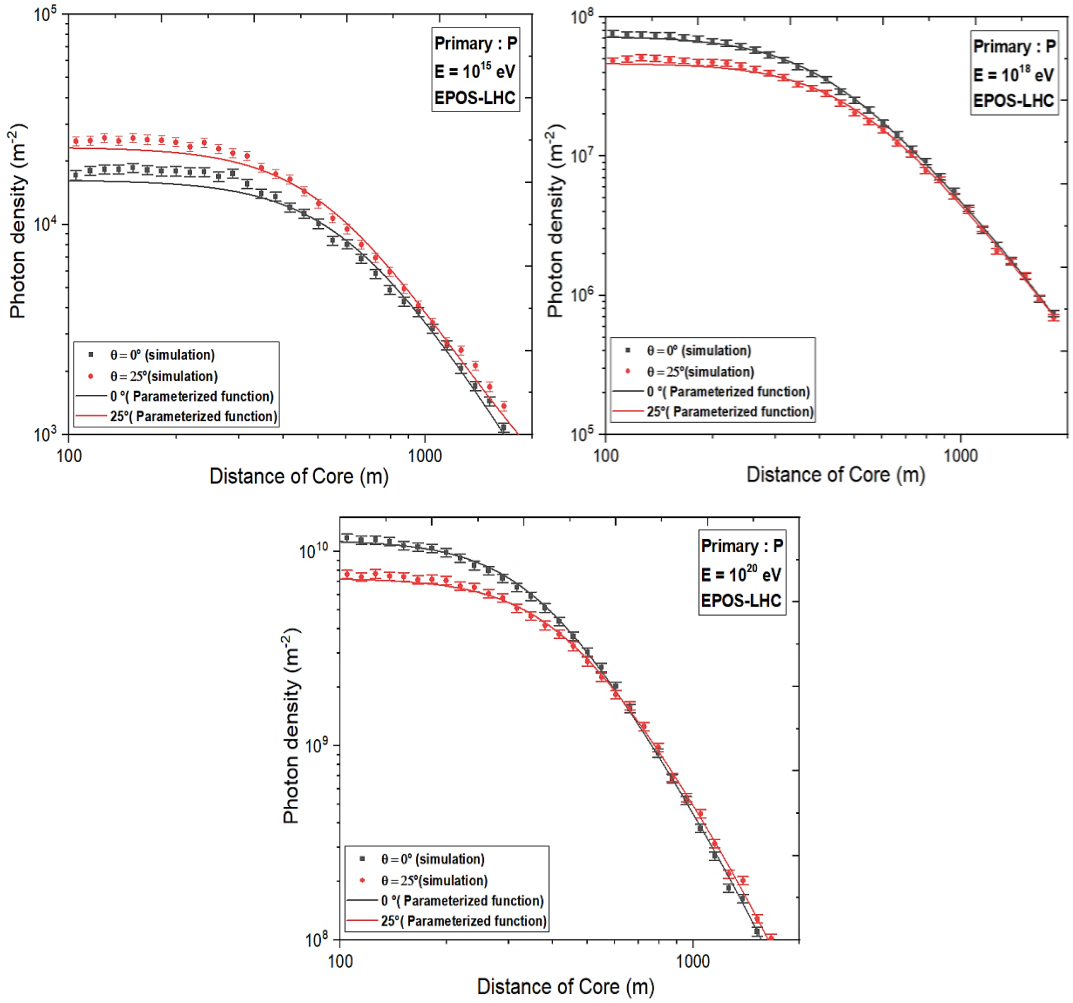

Figure 5. Lateral Distribution of photon density at (0° and 25°) and (10^{15}, 10^{18},10^{20}) eV Simulation by AIRES Using EPOS-LHC (Symbols), and parameterization Logistic Functions (solid lines) resulting from eq. (5)

Table 1. Logistic function coefficients at vertical and inclined EAS, Eq. (5) was developed to parameterize the AIRES simulation for proton primary particles with energy 10^{15} eV.

Primary Particles	Created Radiation	θ	Values of Coefficients				R^2	SD (Photon/m^2)	Mean (Photon/m^2)
			α	λ	η	β			
proton	γ	0°	7.27	1135855.96	404.19	3.27	0.99218	2.92×10^7	4.25×10^7
		25°	4.68	1449784.78	467.14	3.64	0.97819	1.86×10^7	2.94×10^7

Table 2. Logistic function coefficients at vertical and inclined EAS, Eq. (5) was developed to parameterize the AIRES simulation for proton primary particles with energy 10^{18} eV.

Primary Particles	Created Radiation	θ	Values of Coefficients				R^2	SD (Photon/m^2)	Mean (Photon/m^2)
			α	λ	η	β			
p	γ	0°	16594.28	1556.44	556.63	4.03	0.9426	6195.52	11561.56
		25°	23499.56	1861.90	512.57	3.96	0.96151	8980.65	15776.30

Table 3. Logistic function coefficients at vertical and inclined EAS, Eq. (5) was developed to parameterize the AIRES simulation for proton primary particles with energy 10^{20} eV.

Primary Particles	Created Radiation	θ	Values of Coefficients				R^2	SD (Photon/m^2)	Mean (Photon/m^2)
			α	λ	η	β			
p	γ	0°	1.16	4810033.79	350.70	3.01	0.99756	4.69×10^9	6.27×10^9
		25°	7.26	1.30	425.06	3.48	0.99112	2.93×10^9	4.35×10^9

Conclusion:

The association between the lateral distribution function (LDF) and the energy of cosmic rays in the ankle and knee regions is an important topic in the research of ultra-high-energy cosmic rays. The LDF illustrates how the density of photons produced in extensive air showers (EAS) changes with lateral distance from the shower axis. The energy reconstruction in the knee region is dependent on precisely simulating the LDF, as shower development. is influenced by the primary particle's mass and energy. In the ankle region, the LDF becomes less susceptible to composition and controls by primary energy. The LDF in this region used for restoring the energy of the primary cosmic ray, often by measuring the signal at a certain lateral distance, 1000 m from the core. The energy resolution in this region is generally better than in the knee region because the showers are well-developed and the LDF is less affected by fluctuations.

Acknowledgments

For essential support, the authors are grateful to Mustansiriyah University in Baghdad, Iraq (www.uomustansiriyah.edu.iq). They also express their gratitude to the inventors of the Aires system for their assistance and suggestions in making this endeavor possible.

References

1. The Pierre Auger Collaboration, Nucl. Instrum. Methods Phys. Res. **798** (2015)
2. I F Hussein and A A Al-Rubaiee, Malaysian J. Sci. **33** (2022) 74.
3. P Sommers, C R Physique **5** (2004) 463.
4. A. N. Cillisa and S. J. Sciuttob, *Phys. Rev.* **64** (2001) 013010.
5. I F Hussein, A A Al-Rubaiee, et al., Nucl. Phys. **33** (2024).
6. A M Hillas, Acta Phys. Acad. Sci. Hung. **29**(Suppl. 3), (1970) 360.
7. A Obermeier, Forschungszentrum Karlsruhe GmbH, FZKA **7284** (2007).
8. G V Kulikov and G B Khristiansen, Semantic Scholar (1963).
9. J H Buckley, C W Akerlof, et al., Astron. Astrophys. **329** (1998) 639.
10. B Bartoli, P Bernardini, et al., Phys. Rev. D **91** (2015) 112017.
11. Z You, S Zhang, et al. (LHAASO), Proc. 38th Int. Cosmic Ray Conf. (ICRC2023).
12. F Varsi, S Ahmad, et al. (GRAPES-3), Proc. XXIV DAE-BRNS High Energy Phys. Symp., **277** (2022) 649.
13. V V Prosin, S F Berezhnev, et al., Nucl. Instrum. Methods Phys. Res. A **756** (2014) 94.
14. K F Fadhel, A A Al-Rubaiee, et al., J. Phys. **2386** (2021).
15 Li Xinlong, Tianlu Chen, CC BY 4.0 License (2023).
16. A Geraniosi, E Fokitis, et al., Proc. 30th Int. Cosmic Ray Conf. (2008).
17. A A Al-Rubaiee, U Hashim, et al., Serb. Astron. J. **190** (2015) 79.
18. A A Al-Rubaiee, Astrophys. Astron. **35** (2014) 631.
19. R I Raikin, A A Lagutin, et al., Proc. Int. Cosmic Ray Conf. (ICRC 2001)
20. K Greisen, Ann. Rev. Nucl. Sci. **10** (1960) 63.
21. B K Lubsandorzhiev, Nucl. Instrum. Methods Phys. Res. A **595** (2008) 73.
22. A A Al-Rubaiee, O A Gress, et al., Russ. Phys. J. **48** (2005) 1004.
23. B A Chartres, H Messel, Phys. Rev. **104** (1956) 517.
24. T Stanev, High Energy Cosmic Rays, Springer, Heidelberg.**462** (2010).
25. I F Hussein, A A Al-Rubaiee, AIP Conf. Proc. **2591** (2023) 030072.
26. A V Glushkov, A Saburov, Phys. Atom. Nucl. **82** (2019) 663.
27. I F Hussein, A A. Al-Rubaiee, Al-Mustansiriyah J. Sci. **33** (2022).
28. J Matthews, Astropart. Phys. **22** (2005) 387.
29. T K Gaisser, R Engle, et al., Cosmic Rays and Particles Physics (2nd ed.), Cambridge University Press (2016) 444
30. S Hayakawa, Cosmic Ray Physics: Nuclear and Astrophysical Aspects, Vol. 22, Interscience Monographs (1969).
31. D Heck, J Knapp, et al., CORSIKA: A Monte Carlo code to simulate extensive air showers .FZKA Report 6019 (1998).
32. G Atreidis, EPJ Web Conf. **137** (2017) 13001.
33. S J Sciutto, AIRES: User's Guide and Reference Manual, Technical Report (2019).